

3rd CIRP Conference on BioManufacturing

Modeling and additive manufacturing of biomimetic heterogeneous Scaffold

Sameer Kale^c, Navid Khani^{a,b}, Ali Nadernezhad^{a,b}, Bahattin Koc^{a,b,*}

^aFaculty of Engineering and Natural Sciences, Sabanci University, Istanbul, Turkey

^b3D Bioprinting Laboratory, Sabanci University Nanotechnology Research and Application Center, Istanbul, Turkey

^cIndustrial Engineering, University at Buffalo, SUNY, Buffalo, USA

* Corresponding author. Tel.: +90-216-483-9557; fax: +90-216-483-9550. E-mail address: bahattinkoc@sabanciuniv.edu

Abstract

In this paper, a feature-based bio-CAD modeling of three-dimensional tissue scaffolds by considering spatial distribution of biologically active materials is presented for biomufacturing and tissue engineering applications. Proposed model is based on uniform distribution of bio-active particles in different regions of scaffold, which is constrained by geometrical and biological features. The proposed method was integrated with a recently developed method of multi-material additive manufacturing of hydrogel structures, for bio-additive manufacturing of the heterogeneous scaffolds. 3D bioprinted heterogeneous scaffolds were provided as an example for physical implementation of developed algorithm to validate the model.

© 2016 The Authors. Published by Elsevier B.V. This is an open access article under the CC BY-NC-ND license (<http://creativecommons.org/licenses/by-nc-nd/4.0/>).

Peer-review under responsibility of the scientific committee of the 3rd CIRP Conference on BioManufacturing 2017

Keywords: Scaffold, Biomimetic, Heterogeneous additive manufacturing;

1. Introduction

Tissue engineering is a complex process where a porous scaffold with or without cells is used to heal or regenerate the targeted tissue. The sequence of events is guided by a series of growth factors, cytokines, cell-cell and cell-matrix interactions. To imitate nature's healing environment, these scaffolds must incorporate vital growth factors or proteins that are able to act on cell migration, differentiation, proliferation and organization in a functional tissue. These growth factors are polypeptides that transmit signals to modulate cellular activities. Thus, proliferation and other behaviors of cells on advanced bio-specific materials can be controlled by incorporating a controlled release of bioactive particles, such as natural growth factors, hormones, enzymes or synthetic cell cycle regulators [1]. These bioactive particles will deliver the appropriate, necessary cues in a controlled spatial and temporal fashion to improve healing or tissue regeneration. However, a major challenge lies in developing efficient delivery mechanisms to

mimic the in vivo release profiles of growth factors produced during natural tissue morphogenesis or repair [2].

In the literature, several heterogeneous object modeling techniques have been proposed for solid modeling of consumer products: the r_m -object approach is used for representing heterogeneous objects by Kumar and Dutta [3]. This method represents the material variation as functions of spatial position relative to a reference entity and material variations were assumed to be given a priori. Samanta and Koc [4] have proposed feature based heterogeneous object modeling using B-spline surfaces and B-spline volumes to represent 2D and 3D-dependent material distributions using the same set of control points for both the geometries and the material compositions. Weiss et al [5] have presented a Bayesian methodology for computer-aided experimental design of heterogeneous fibrin-based scaffolds having spatial distribution of growth factors designed to induce and direct the growth of new tissue as the scaffold degrades.

However, these heterogeneous object modeling techniques assume a continuous variation of materials throughout the designed object, whereas in tissue scaffolds bioactive particles

are discrete entities and need to be spatially distributed in a controlled manner within the porous scaffold. Af

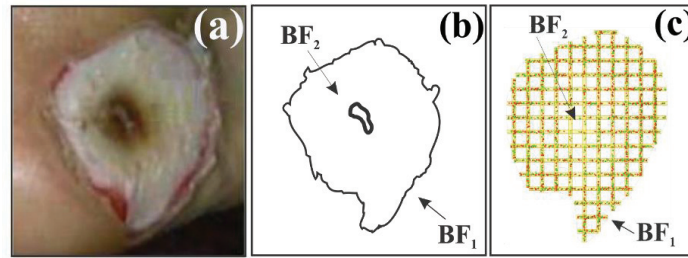


Fig. 1. Overall procedure of modeling and design of biomimetic tissue scaffold

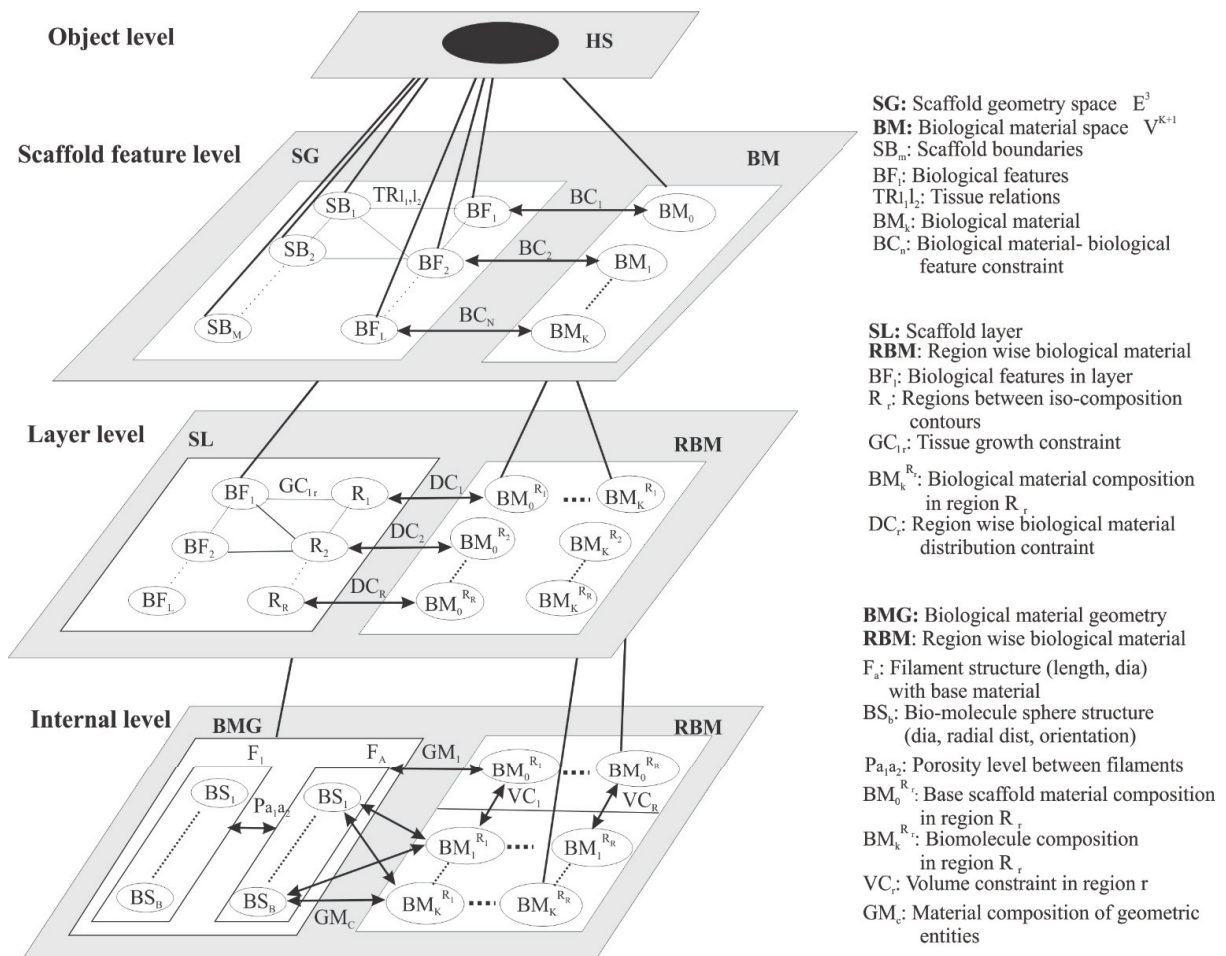


Fig. 2. Feature based heterogeneous scaffold model hierarchy

Hence, the existing heterogeneous object modeling techniques cannot be directly used in modeling of tissue scaffolds with controlled distribution of bioactive particles.

During the past decade, extensive studies on multi-material additive manufacturing by using multi-nozzle deposition systems were resulted in numerous reports on fabrication of heterogeneous scaffolds addressed to be used in biomedical

applications [6-8]. However, there are still concerns about the precision of spatial distribution of multi-material segments in fabricated object, especially in controlling the structural integrity of printed constructs. Single nozzle deposition systems were developed to provide a solution [9-11], but they have been often resulted in formation of the transient sections and lack of control in continuity of functionality of neighboring regions, due to the mixing of consequent materials during deposition. This problem becomes more evident when these designs were intended to be used in deposition of considerably small regions of materials with altering features. We developed a method [12] to fabricate heterogeneous 3D structures with precise control the functionality of multi-material segments while the structural integrity and continuity could be preserved during the printing. In this paper, this method was used to implement the developed algorithm to ensure that the design criteria were implemented in a controllable manner.

In order to better mimic aspects of nature or to enable biologically inspired engineered designs, new scaffold design and fabrication methods must include heterogeneous compositions incorporating controlled spatial distributions of cells, growth factors, and proteins. In this paper, a novel biomimetic model that uses feature based design technique for complex and irregular growth factor heterogeneities in scaffolds is proposed. This new design technique will allow simultaneous deposition of biomaterials and bioactive particles along with biomimetic placements of cells and proteins within 3D scaffold structures. Using the shape of tissue regeneration area, heterogeneous scaffold that will mimic the release profiles of growth factors produced during natural tissue morphogenesis or tissue repair are modelled. This paper is organized as follows: the feature-based biomimetic modelling of scaffolds is discussed in section 2. Biomimetic design of scaffolds with growth factors is explained in Section 3. Implementation of developed algorithm is presented in section 4.

2. spatially controlled growth factor distribution

The overall procedure for feature based biomimetic modeling of heterogeneous scaffolds is shown in Fig. 1. A wound model which is used through this presentation is shown in Fig. 1(a). Three-dimensional model is constructed using proper image processing methods Fig. 1(b) and segmentation. After obtaining the 3D model of healing area, biological features that will govern the spatial distribution of growth factors are identified. Further, the heterogeneous scaffold is modeled with biologically active particle distribution across each layer of scaffold as seen in Fig. 1(c).

In this research, a feature-based representation model of heterogeneous scaffold with spatially controlled bioactive particle distribution is presented. The heterogeneous scaffold model hierarchy is shown in Fig. 2. A feature based representation scheme is used to represent heterogeneous scaffold with bioactive particles distributed between biological features. The heterogeneous scaffold **HS** composed of K biological materials BM_1, BM_2, \dots, BM_K is modeled as follows:

$$\mathbf{HS} = (\mathbf{SG}, \mathbf{TR}, \mathbf{BM}, \mathbf{BC})$$

$$\begin{aligned} \mathbf{SG} &= \{\{SB_m\}, \{BF_l\}\}, m = 1, \dots, M; l = 1, \dots, L \quad \mathbf{SG} \in E^3 \\ \mathbf{TR} &= \{TR_{l_1, l_2}\}, l_1 = 1, \dots, L; l_2 = 1, \dots, L; l_1 \neq l_2 \\ \mathbf{BM} &= \{BM_k, f_k(g)\}, k = 0, \dots, K \quad \mathbf{BM} \in V^{K+1} \\ \mathbf{BC} &= \{BC_n\}, n = 1, \dots, N \end{aligned} \quad (1)$$

where, E^3 is the three-dimensional Euclidean space and V^{K+1} is the $(K + 1)$ -dimensional biological material space. In order to facilitate the design of heterogeneous scaffold consisting of varying bioactive particle distribution, biological entities are used as biological features. By selecting proper biological entities as the reference features and specifying a bioactive particle distribution function across the features, the distribution information can be incorporated with biological feature information. The biological feature can be an arbitrary feature of the tissue regeneration volume in the geometric form of a point, curve, surface or the entire boundary of the biological object [13]. In this way, the natural tissue regeneration process between the two wound features can be imitated. These features are represented by set $\{BF_l\}$ termed as collection of L biological features BF_1, BF_2, \dots, BF_L . The biological features are the specific shapes of the tissue regeneration area and contribute to the formation of the boundary of final scaffold geometry.

scaffolds must be represented in 3D space. After wound volume are obtained using image processing techniques, the scaffold geometry **SG** is represented as set of scaffold boundaries $\{SB_m\}$, $m = 1, \dots, M$ and set of biological features $\{BF_l\}$, $l = 1, \dots, L$. Each of the scaffold boundaries SB_m are modeled as NURBS surfaces of two parameters u and v mapped into Euclidean space E^3 . A NURBS surface SB_m can be expressed as:

$$SB_m(u, v) = \frac{\sum_{i=0}^I \sum_{j=0}^J N_{i,p}(u) N_{j,q}(v) w_{i,j} P_{i,j}}{\sum_{i=0}^I \sum_{j=0}^J N_{i,p}(u) N_{j,q}(v) w_{i,j}} \quad (2)$$

where, $P_{i,j} = (x_{i,j}, y_{i,j}, z_{i,j})$ and $w_{i,j}$ are weights of each $P_{i,j}$. $N_{i,p}(u)$, $N_{j,q}(v)$ are the B-spline basis functions defined on the knot vectors, U and V , with degree p and q respectively. The biological features are part of scaffold geometry and scaffold boundaries. Therefore, relation of biological feature BF_l with other biological features is maintained in the tissue relation set $\mathbf{TR} = \{TR_{l_1, l_2}\}$, $l_1 = 1, \dots, L; l_2 = 1, \dots, L; l_1 \neq l_2$.

The $K + 1$ biological materials are elements of biological material set **BM** defined in heterogeneous scaffold. For biomimetic design, it is assumed that the tissue regeneration starts from one biological feature and closes towards another biological feature. So, the bioactive particles required for tissue regeneration are assumed to vary in only one direction (g) i.e. from one biological feature to another biological feature. This distribution of growth factors or proteins in micro-particles from one biological growth factors to another is represented by one-dimensional parametric function $f_k(g)$, where $k = 0, \dots, K$. Each element of **BM** contains the biological material type BM_k and their one dimensional mathematical form of variation $f_k(g)$, where $k = 0, \dots, K$. Hence, **BM** belongs to $(K + 1)$ -dimensional biological material space. Further, the biological material BM_0 is considered as the biodegradable

scaffold material and the biological material type BM_k , $k = 1, \dots, K$ are considered as bioactive particles (growth factors or proteins). In tissue engineering, the bioactive micro-particle release rate should be varied as per desired distribution in order to bio-mimic healing process. So the biological material distribution functions $f_k(g)$ are constrained with at least one biological feature BF_l and are given by set $BC = \{BC_n\}$, $n = 1, \dots, N$. In other words, these biological material distribution functions constraints by tissue regeneration directions. In Fig. 3, bioactive particles BM_k are distributed along one direction between biological features BF_1, BF_2 . The bioactive particles BM_k are distributed as given by function $f_k(g)$. Similarly, different types of growth factors BM_k , each having different distribution function $f_k(g)$ could be constrained between biological features BF_l and the biological constraint is given by BC_n . Fig. 4 shows one dimensional distribution of bioactive particles between different biological features.

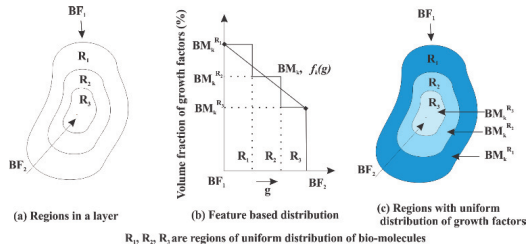


Fig. 3. Different regions and growth factor distribution in a layer.

For bioprinting of the designed scaffold, the heterogeneous scaffold is modeled as set of layers. So, feature level representation is decomposed into layer level representation that uses the scaffold geometry information and biological material information at each layer. The set of layers is given by $L = \{L_h\}$, $h = 1, \dots, H$. Each layer L_h at height z_h represents scaffold geometric information and biomaterial information decomposed from feature level into discrete layers as per design requirements. Each L_h satisfies the relation:

$$L_1 \cap L_2 \dots \cap L_H = \emptyset \quad (3)$$

The height z_h is determined using the porosity level $P_{h,h+1}$, $h = 1, \dots, H$ between any two layers required in heterogeneous scaffold. A layer L_h can be represented as follows:

$$\begin{aligned} L_h &= (\mathbf{SL}, \mathbf{GC}, \mathbf{RBM}, \mathbf{DC}, \mathbf{LC}) \\ \mathbf{SL} &= \{\{BF_l\}, \{R_r\}\}, l = 1, \dots, L; r = 1, \dots, R \\ \mathbf{GC} &= \{GC_{l,r}\}, l = 1, \dots, L; r = 1, \dots, R \\ \mathbf{RBM} &= \{BM_k^{R_r}\}, k = 1, \dots, K; r = 1, \dots, R \\ \mathbf{DC} &= \{DC_r\}, r = 1, \dots, R \\ \mathbf{LC} &= \{P_{h,h+1}\}, h = 1, \dots, H \end{aligned} \quad (4)$$

In each scaffold layer L_h , the set \mathbf{SL} consists of geometric information of scaffold. Set \mathbf{SL} consists of biological features $\{BF_l\}$, $l = 1, \dots, L$ and biological material distribution regions given by $\{R_r\}$, $r = 1, \dots, R$. These regions represent the tissue regeneration areas over which growth factor release rates have

to be controlled during natural tissue morphogenesis or tissue repair. In each layer, this tissue repair occurs from different biological features BF_l and follows through the regions R_r . The tissue growth constraint $GC_{l,r}$, $l = 1, \dots, L$; $r = 1, \dots, R$ in set \mathbf{GC} represents topological positions of each region R_r with respect to biological feature BF_l . In each layer, the different biological particle change boundaries $Re(u)$ between each region R_r are modeled as p^{th} degree NURBS curve given by:

$$Re(u) = \frac{\sum_{i=0}^l N_{i,p}(u) w_i Q_i}{\sum_{i=0}^l N_{i,p}(u) w_i} \quad (5)$$

where, $Q_i = (x_i, y_i, z_i)$ are control points of curve obtained by curve fitting with weights w_i and $N_{i,p}(u)$ are the B-spline basis functions defined on the knot vectors, U .

Further, within each region R_r the composition of biological material BM_k is given by $BM_k^{R_r}$, $k = 0, \dots, K$; $r = 1, \dots, R$. In this way, the biological material distribution in each layer is represented by region wise biological material composition \mathbf{RBM} . The biological materials compositions $BM_k^{R_r}$ are constrained using set of distribution constraints \mathbf{DC} in each region R_r inside scaffold geometry. The distribution constraint maintains the distribution requirements of biological material composition $BM_k^{R_r}$ in each region R_r such that each biological material BM_k is properly distributed as per distribution function. Further, each scaffold layer L_h is separated from adjacent layers L_{h+1} to maintain a given porosity level \mathbf{LC} given by $P_{h,h+1}$, $h = 1, \dots, H$. This layer level representation is explained in Fig. 3.

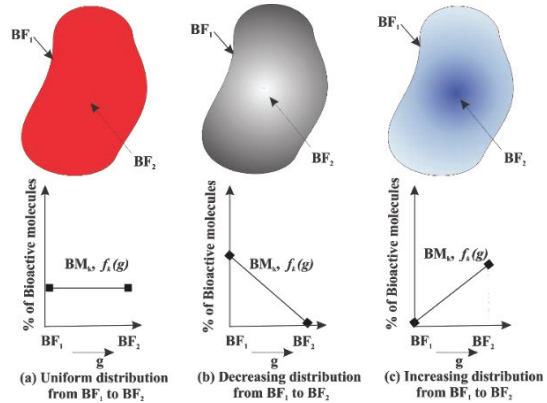


Fig. 4. One-dimensional bioactive particle distribution between different biological features.

In order to model the heterogeneous scaffold with biological materials and desired porosity level, each scaffold layer is designed with several biodegradable material or hydrogel filaments with bioactive particles. The collection of E filaments \mathbf{FL}_e in each layer is given by $\mathbf{FL} = \{\mathbf{FL}_e\}$, $e = 1, \dots, E$. The set \mathbf{FL}_e consists of structural and material information of base scaffold material and bioactive particles in scaffold and constraint of volume fraction between them. Each filament \mathbf{FL}_e is modeled as follows:

$$\mathbf{FL}_e = (\mathbf{BMG}, \mathbf{RBM}, \mathbf{VC}, \mathbf{PC}, \mathbf{O})$$

$$\begin{aligned}
 \mathbf{BMG} &= \{F_a(\text{length, diameter}), BS_b(\text{diameter, radial distance, orientation}), \\
 &\quad a = 1, \dots, A; b = 1, \dots, B \\
 \mathbf{RBM} &= \{BM_k^{R_r}, k = 1, \dots, K; r = 1, \dots, R \\
 \mathbf{VC} &= \{VC_r: \sum_{k=0}^K BM_k^{R_r} = 1\}, r = 1, \dots, R \\
 \mathbf{PC} &= \{P_{a,a+1}\}, a = 1, \dots, E - 1 \\
 \mathbf{O} &= \{\tau_{h,h+1}\}, h = 1, \dots, H
 \end{aligned} \tag{6}$$

The geometric information of biological materials (biodegradable scaffold material and bioactive particles) in each filament \mathbf{FL}_e is stored in set \mathbf{BMG} . Considering that biological materials have regular geometric shapes, the biodegradable scaffold material BM_0 is modeled as a filament $F_a(\text{length, diameter})$ with cylindrical shape having (length, diameter) as two parameters to represent its shape. Similarly, the bioactive micro-particles with growth factors or proteins $BM_k, k = 1, \dots, K$ represented as $BS_b(\text{diameter, radial distance, orientation})$ and are assumed to be of spherical shape with parameters as (diameter, radial distance, and orientation) within each filament \mathbf{FL}_e . The region wise biological material composition set \mathbf{RBM} is used to represent the composition of biological material BM_k within each region R_r the filament \mathbf{FL}_e passes through. Within each region R_r of filament \mathbf{FL}_e the composition of biological material BM_k is given by $BM_k^{R_r}, k = 0, \dots, K; r = 1, \dots, R$. In order to maintain the heterogeneity in each region R_r of the scaffold layer, the biological materials BM_k must satisfy the volume constraints given by VC_r in set \mathbf{VC} such that $\sum_{k=0}^K BM_k^{R_r} = 1, r = 1, \dots, R$. Also, to maintain the porosity in each layer, we represent the porosity level $\mathbf{PC} = \{P_{a,a+1}\}, a = 1, \dots, E - 1$ between any two adjacent filaments \mathbf{FL}_a and \mathbf{FL}_{a+1} . Further, the filaments in a particular layer at height h are oriented with filaments of layer at height $h + 1$ by $\tau_{h,h+1}$. This set of orientation $\mathbf{O} = \{\tau_{h,h+1}\}, h = 1, \dots, H$ will also decide the porosity level between any two adjacent layers.

Fig. 5 shows an example of internal architecture of a layer. The filament \mathbf{FL}_1 and \mathbf{FL}_2 are separated to maintain porosity level $P_{1,2}$. Between the biological features BF_1 and BF_2 , biological material is distributed in regions given by R_1, R_2, R_3 . In this example, the biodegradable scaffold material BM_0 is modeled as a filament of cylindrical shape and the bioactive particles (growth factors or proteins) BM_1, BM_2 are modeled as spherical shapes.

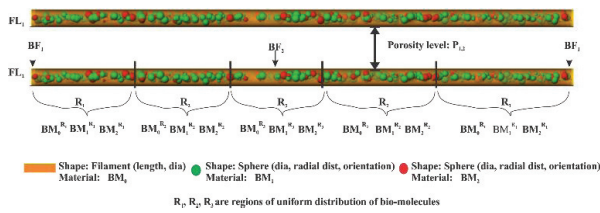


Fig. 5. Internal architecture of a layer made with biodegradable material (filaments), growth factors (spheres), and porosity level.

3. Biomimetic design of scaffolds with bioactive particles

In previous section, feature based heterogeneous scaffold model hierarchy was presented and bioactive particle distribution between different biological features was

illustrated. In this section, the methodology for biomimetic design of scaffolds with bioactive particles by obtaining three dimensional CAD model of tissue construct and the biological features is discussed.

3.1. Biological feature recognition

In order to facilitate the design of heterogeneous scaffold consisting of varying bioactive particle distribution, biological entities are used as biological features. By selecting proper biological entities as the reference features and specifying a particle distribution function across the features, distribution information can be incorporated with biological feature information. The process to obtain biological features from the tissue region is discussed below.

Our aim is to reconstruct the three-dimensional structure of the tissue regeneration volume from image data. Fig. 6, shows the steps involved in construction of 3D CAD model of tissue construct to be fabricated. Noninvasive imaging techniques could be used for biological feature recognition. Thin-slice computer tomography (CT) imaging, micro CT imaging, contrast-enhanced MRI, micro MRI and digital photography are some of the techniques that offer a noninvasive quantitative assay for the wound imaging[14]. The image acquisition system must preserve as much information of tissue regeneration area as possible.

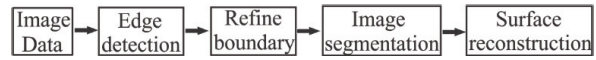


Fig. 6. Overview of entire image reconstruction

3.2. Scaffold matrix modeling

After the 3D reconstruction of the image is obtained, the outer surface boundaries of the 3D CAD model are used as scaffold boundaries represented with set of scaffold boundaries $\{SB_m\}, m = 1, \dots, M$ and $SB_m(u, v)$ are represented as NURBS surfaces using Equations (2). This surface model $SB_1(u, v)$ is sliced into layers to decompose it into planar curves or scaffold boundary $Cb(u)$. This information from sliced layered plane is used in an ordered sequence during fabrication process. The slicing thickness parameter z_h is used to decompose the 3D volume. The set \mathbf{L} is introduced to indicate the discrete layers into which surface model is decomposed.

$$\mathbf{L} = \{\mathbf{L}_h: \mathbf{L}_1 < \mathbf{L}_2 < \dots < \mathbf{L}_{H-1} < \mathbf{L}_H\}, h = 1, \dots, H \tag{7}$$

where \mathbf{L}_h represents the h^{th} decomposed layer.

After slicing, in each layer \mathbf{L}_h , the scaffold boundary $Cb_{L_h}(u)$ is modeled as p^{th} degree NURBS curve given by:

$$Cb_{L_h}(u) = \frac{\sum_{i=0}^I N_{i,p}(u) w_i \mathbf{C}_i}{\sum_{i=0}^I N_{i,p}(u) w_i} \tag{8}$$

where, $C_i = (x_i, y_i, z_i)$ are control points of curve obtained by curve fitting with weights w_i and $N_{i,p}(u)$ are the B-spline basis functions defined on the knot vectors U .

By decomposing the surface model, each layer can be modeled and fabricated using solid free form fabrication method, as seen in Fig. 7. A 3D reconstruction of image along with biological features BF_1 and BF_2 is shown in Fig. 7(a). This 3D CAD model consists of scaffold boundaries $SB_1(u, v)$ and $SB_2(u, v)$. To model the 3D porous scaffold structure, the outer surface $SB_1(u, v)$ is sliced at different heights z_h and decomposed in layer L_h as shown in Fig. 9(b). Further, a scaffold boundary $Cb_{L_h}(u)$ as seen in Fig. 7(c) is obtained after slicing a surface with parallel planes. Fig. 7(d) shows modeled porous layers with biodegradable material filaments using scaffold boundaries $Cb_{L_h}(u)$. After stacking such several layers along a build direction, 3D scaffold structure is obtained as seen in Fig. 7(e). The build direction is chosen such that the scaffold structure can withstand the weight of top layers by its own without any need of extra support material. Note that the scaffold model consists of simply the biodegradable material matrix and there are no bioactive particles in it.

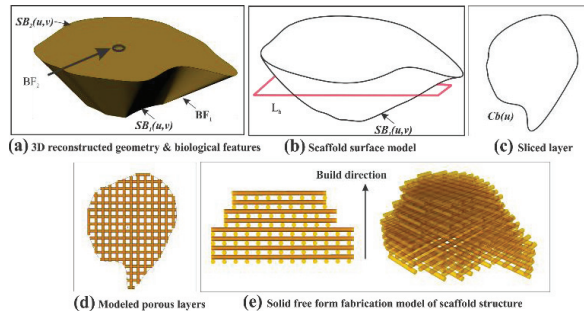


Fig. 7. Scaffold model without any bioactive particles

3.2 Spatial bioactive particle variation

In the previous sections, biological features, 3D reconstructed geometry and scaffold structures are obtained from the tissue reconstruction volume. For biomimetic designs, scaffolds mimic natural tissue structure and seek to replicate all aspects of tissue structure and function. Since tissue formation and repair is a complex cascade of events in which a number of growth factors are involved, controlled delivery of combinations of growth factors from micro-particles embedded in scaffold appear to be a logical strategy in mimicking nature. For bone regeneration, wound healing or blood vessel formation, the tissue formation ideally takes place from healthy tissue area to damaged tissue area. This morphological change from one tissue region to other tissue region can be seen as steps of tissue growth and it requires appropriate growth factors to be released from scaffolds in spatial and temporal fashion. By imitating this tissue regeneration sequence, the growth factor, protein variation across biological features of tissues can be estimated by means of volume lofting method. This section discusses the methodology of obtaining spatial bioactive particle variation across biological features in order to imitate the natural tissue regeneration process.

For using volume lofting method, it is assumed that all the biological features BF_1 , BF_2 are represented as entities such as point or NURBS curves/surfaces. Given any two biological features as geometric surface entities, using volume lofting method, the biological material information is lofted between the features BF_1 and BF_2 . The lofting of NURBS surface along an arbitrary trajectory curve $Tr(g)$ is discussed below. The trajectory of lofting in g direction is denoted by a straight line, given by:

$$Tr(g) = \frac{\sum_{s=0}^S N_{s,t}(g) w_s T_s}{\sum_{s=0}^S N_{s,t}(g) w_s} \quad (9)$$

where, $T_s = (x_s, y_s, z_s)$ and w_s are weights of each T_s . $N_{s,t}(g)$ are the B-spline basis functions defined on the knot vectors, G , with degree t .

The outer tissue boundary or biological boundary BF_1 is modeled as NURBS surface as given by Equation 2:

$$SB_1(u, v) = \frac{\sum_{i=0}^I \sum_{j=0}^J N_{i,p}(u) N_{j,q}(v) w_{i,j} P_{i,j}}{\sum_{i=0}^I \sum_{j=0}^J N_{i,p}(u) N_{j,q}(v) w_{i,j}} \quad (10)$$

where, $P_{i,j} = (x_{i,j}, y_{i,j}, z_{i,j})$ and $w_{i,j}$ are weights of each $P_{i,j}$. $N_{i,p}(u)$, $N_{j,q}(v)$ are the B-spline basis functions defined on the knot vectors, U and V , with degree p and q respectively.

The lofted volume $Lv(u, v, g)$ is obtained by lofting biological boundary $SB_m(u, v)$ along the straight line $Tr(g)$. Thus, lofted volume $Lv(u, v, g)$ of degree (p, q, t) with parameters u, v, g and knot sequence U, V, G is given as:

$$Lv(u, v, g) = \frac{\sum_{i=0}^I \sum_{j=0}^J \sum_{s=0}^S N_{i,p}(u) N_{j,q}(v) N_{s,t}(g) w_{i,j,s} P_{i,j,s}}{\sum_{i=0}^I \sum_{j=0}^J \sum_{s=0}^S N_{i,p}(u) N_{j,q}(v) N_{s,t}(g) w_{i,j,s}} \quad (11)$$

The regions between lofted volumes represent morphological change from one tissue region to other tissue region and hence the continuous bioactive particles (with growth factors or proteins) composition change between different biological features. Creating a large number of lofted volume regions at parametric distance g will give a smooth variation of bioactive particles changing between the biological features. This lofted volume information will be used for mapping the 3D bioactive particle composition variation into 2D plane for modeling and fabrication purpose.

An example of 3-D wound closure direction and the lofted volume is shown in Fig8. In case of open wound healing, contraction phenomenon is observed. Contraction is the process in which the surrounding skin is pulled circumferentially toward the wound [15]. After generating the 3D surface data of wound, the outer surface $SB_1(u, v)$ is assigned as a biological feature BF_1 and then the innermost region projected on top surface as second biological feature BF_2 . The wound closure is assumed to follow the path from outer surface to top surface and the morphological change from biological feature BF_1 to BF_2 is obtained using volume lofting operation discussed using Equations 9 to 11. The surface $SB_1(u, v)$ is lofted along $Tr(g)$ direction to obtain 3D lofted volume (Fig 8(a)). Each of the regions in lofted volume are separated by parametric distance g from biological feature BF_1 . For illustration purpose, between the features BF_1

and BF_2 , the lofted volume regions with varying growth factor composition are shown as R_1, R_2, R_3, R_4, R_5 .

Figure 8(b) shows a one-dimensional variation $f_k(g)$ of bioactive particle BM_k parameterized between the biological features BF_1 and BF_2 . The bioactive particle requirements for each lofted volume regions can be obtained by using the parametric distance g from biological feature BF_1 .

The lofted volume is decomposed into discrete layers using slicing. The slicing thickness parameter z_h is used to decompose the 3D volume. A set L given by Equation 7 is introduced to indicate the discrete layers into which surface model is decomposed. In each layer, the different bioactive particles change boundaries $Re(u)$ between each region R_r are modeled as p^{th} degree NURBS curve given by Equation 5.

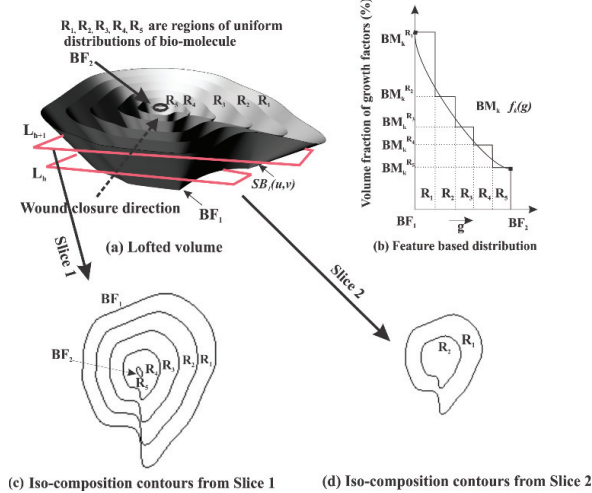


Fig. 8. Wound closure in 2D plane

Figure 8(a) shows the lofted volume sliced at different heights. In slice 1, five different regions can be seen, each region having distribution of bioactive particles, obtained by slicing the lofted volume as shown in Fig 8(c). Similarly, in slice 2 (Fig 8(d)), two different regions are shown are slicing lofted volume.

Considering Fig. 8(c), five different regions R_1, R_2, R_3, R_4, R_5 represents the regions over which tissue repair progresses from biological feature BF_2 to BF_1 . Fig. 8(b) shows the distribution of growth factor BM_k that is required between the biological features BF_1 and BF_2 and is given by function $f_k(g)$. Using the parametric distances of boundaries of regions R_1, R_2, R_3, R_4, R_5 from biological feature BF_k , the composition of growth factor BM_k in each region is obtained as $BM_k^{R_1}, BM_k^{R_2}, BM_k^{R_3}, BM_k^{R_4}, BM_k^{R_5}$ from the distribution function. Finally, the bioactive particles have to be distributed between in each of regions R_1, R_2, R_3, R_4, R_5 so as to follow the distribution function $f_k(g)$. In this way, using lofted volume and distribution functions $f_k(g)$, $k = 1, \dots, K$ constrained between the two biological features, BF_1 and BF_2 , the composition array $BM_k^{R_r}$ is generated using the parametric distance g from biological features.

For more than one type of bioactive particles BM_k , more than one distribution functions $f_k(g)$, $k = 1, \dots, K$ will be needed, where the distribution varies only in one parametric

direction g . Also, based on design requirements, distribution in more than one parametric direction can also be implemented. The micro-particles with growth factor composition in the scaffold case may be first-order continuous or higher[16]. More information and examples about the lofted volume can be found in [4, 17].

4. Implementation and 3D printing of heterogeneous scaffolds for skin tissue engineering

The scaffold design begins with the acquisition of non-invasive images and image processing of appropriate tissue region of interest. Sliced images of the targeted tissue can be obtained by using CT methods. Once the sliced images are obtained, they are imported into ITK-SNAP [18]. ITK-SNAP implements the 3D geodesic active contour method as well as the region competition method for image segmentation. This is followed by a 3D reconstruction of anatomical structure using available software kits like Mimics or ITK-SNAP. For external skin wounds, digital cameras can be used to get high quality images of the region. For the external skin images, image processing was performed on the sample image using MATLAB Image Processing Toolbox.

Once the 3D surface model of tissue was generated, it was imported into Rhinoceros 5.0 software for surface refinement and non-uniform rational B-spline (NURBS) surface generation. Using the 3D surface model, biological features are obtained and iso-surfaces are created by volume lofting operation between biological features. Further, thin slices were created and sliced data were obtained in the form of lofted NURBS curves. In this way the iso-composition contours in each slice were obtained and used for distribution of bioactive particles over the scaffold.

To physically implement the proposed algorithm, we made two major assumptions for the sake of simplicity. First, fluorescent microbeads were incorporated inside a hydrogel matrix instead of real active particles with proteins (Fig. 9 (a)) such a way that low, average, and high concentrations of growth factor volume fractions were represented by red, blue, and transparent colors, respectively. Moreover, we confined the number of regions with uniform functionality to three (Fig. 9 (b)). We used our recently published method [12] of 3D printing for the implementation of algorithm in the previous section. This method is based on an aspiration on demand protocol for assembling of multi-material segments in low viscous state followed by in situ gel formation. Agarose was used as the carrier hydrogel for fluorescent microbeads to be able to make different regions of the 3D printed scaffold visually distinguishable. To prepare the starting materials, 2 wt.% agarose hydrogels were prepared according to the producer's protocol (Sigma, USA) by boiling water bath method. Fluorescent microbeads (Createx Colors, USA) were added to the hydrogels during the preparation to stain each hydrogel region. The multi-region structure was fabricated by the in house developed 3D printer (SU^{3D}) which is shown in Fig 9(c). The 3D printed scaffold with three regions is shown in Fig. 9(d).

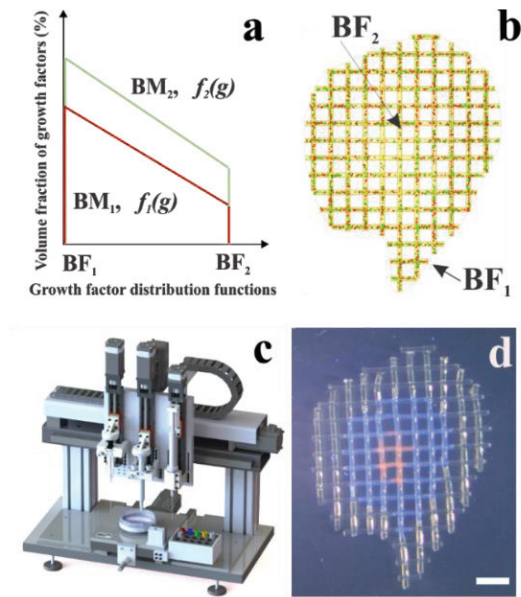


Fig. 9: An example of implemented algorithm for 3D printing of an object with three regions of heterogeneity (scale bar in the printed construct is 4mm)

The advantages of using this method are the high dimensional precision of switching between neighboring regions; ease of material switching due to high accessibility of different inks during the process; and producing constructs with high structural integrity because of using single nozzle design. More details about the process parameters and its features is available at [12].

5. Conclusions

In this paper, feature based modeling of heterogeneous scaffolds is presented for biomimicking the healing process. Using image segmentation methods, 3D model of tissue regeneration volume is obtained. Biological features that control growth factor distribution are identified as features because they dictate the bioactive particle (growth factors or proteins) variation inside a heterogeneous object. These bioactive particles are distributed between biological features using volume lofting method. Based on design requirements, the lofted volume is sliced and each sliced layer is modeled with bioactive particles distributed as per given distribution function. Computational algorithms are developed to vary bioactive particles continuously across the biological features of scaffold. This approach led to achieve a tailored distribution of bioactive micro-particles with growth factors and biological particles based on the demanded release profiles and the biological properties of the modeled tissue constructs. A 3D printed scaffold with three regions is provided as an example for physical implementation of developed algorithm to validate the concept.

References

- [1] R.L. Cleek, K.C. Ting, S.G. Eskin, A.G. Mikos, Microparticles of poly (DL-lactic-co-glycolic acid)/poly (ethylene glycol) blends for controlled drug delivery, *Journal of controlled release* 48(2) (1997) 259-268.
- [2] D.W. Huttmacher, Scaffolds in tissue engineering bone and cartilage, *Biomaterials* 21(24) (2000) 2529-2543.
- [3] V. Kumar, D. Dutta, An approach to modeling & representation of heterogeneous objects, *Journal of Mechanical Design* 120(4) (1998) 659-667.
- [4] K. Samanta, B. Koc, Feature-based design and material blending for free-form heterogeneous object modeling, *Computer-Aided Design* 37(3) (2005) 287-305.
- [5] L.E. Weiss, C.H. Amon, S. Finger, E.D. Miller, D. Romero, I. Verdinelli, L. Walker, P.G. Campbell, Bayesian computer-aided experimental design of heterogeneous scaffolds for tissue engineering, *Computer-Aided Design* 37(11) (2005) 1127-1139.
- [6] D.P. Parekh, D. Cormier, M.D. Dickey, Multifunctional Printing: Incorporating Electronics into 3D Parts Made by Additive Manufacturing, *Additive Manufacturing* (2015) 215.
- [7] B.Y. Ahn, E.B. Duoss, M.J. Motala, X. Guo, S.-I. Park, Y. Xiong, J. Yoon, R.G. Nuzzo, J.A. Rogers, J.A. Lewis, Omnidirectional printing of flexible, stretchable, and spanning silver microelectrodes, *Science* 323(5921) (2009) 1590-1593.
- [8] Y.L. Kong, I.A. Tamargo, H. Kim, B.N. Johnson, M.K. Gupta, T.-W. Koh, H.-A. Chin, D.A. Steingart, B.P. Rand, M.C. McAlpine, 3D printed quantum dot light-emitting diodes, *Nano letters* 14(12) (2014) 7017-7023.
- [9] M. Jafari, W. Han, F. Mohammadi, A. Safari, S. Danforth, N. Langrana, A novel system for fused deposition of advanced multiple ceramics, *Rapid Prototyping Journal* 6(3) (2000) 161-175.
- [10] J.O. Hardin, T.J. Ober, A.D. Valentine, J.A. Lewis, Microfluidic printheads for multimaterial 3D printing of viscoelastic inks, *Advanced Materials* 27(21) (2015) 3279-3284.
- [11] C. Chimate, B. Koc, Pressure assisted multi-syringe single nozzle deposition system for manufacturing of heterogeneous tissue scaffolds, *The International Journal of Advanced Manufacturing Technology* 75(1-4) (2014) 317-330.
- [12] A. Nadernezhad, N. Khani, G.A. Skvortsov, B. Toprakhisar, E. Bakirci, Y. Menciloglu, S. Unal, B. Koc, Multifunctional 3D printing of heterogeneous hydrogel structures, *Scientific Reports* 6 (2016) 33178.
- [13] K. Samanta, B. Koc, Heterogeneous object design with material feature blending, *Computer-Aided Design and Applications* 1(1-4) (2004) 429-437.
- [14] C. Alemdaroglu, Z. Degim, N. Celebi, F. Zor, S. Ozturk, D. Erdogan, An investigation on burn wound healing in rats with chitosan gel formulation containing epidermal growth factor, *Burns* 32(3) (2006) 319-327.
- [15] J. Norton, R.R. Bollinger, A.E. Chang, S.F. Lowry, *Surgery: basic science and clinical evidence*, Springer 2012.
- [16] S.J. Peter, L. Lu, D.J. Kim, G.N. Stamatias, M.J. Miller, M.J. Yaszemski, A.G. Mikos, Effects of transforming growth factor $\beta 1$ released from biodegradable polymer microparticles on marrow stromal osteoblasts cultured on poly (propylene fumarate) substrates, *Journal of biomedical materials research* 50(3) (2000) 452-462.
- [17] K. Samanta, I.T. Ozbolat, B. Koc, Optimized normal and distance matching for heterogeneous object modeling, *Computers & Industrial Engineering* 69 (2014) 1-11.
- [18] P.A. Yushkevich, J. Piven, H.C. Hazlett, R.G. Smith, S. Ho, J.C. Gee, G. Gerig, User-guided 3D active contour segmentation of anatomical structures: significantly improved efficiency and reliability, *Neuroimage* 31(3) (2006) 1116-1128.